ELSEVIER

International Journal of Mass Spectrometry 207 (2001) 1–12

International Journal of Mass Spectrometry

Time-of-flight mass spectrometric detection of mono- and di-substituted benzenes at parts per million concentrations by way of liquid microjet injection and laser ionisation

Wendy L. Holstein, Margaret R. Hammer, Gregory F. Metha, Mark A. Buntine*

Department of Chemistry, University of Adelaide, Adelaide, SA 5005 Australia

Received 5 September 2000; accepted 1 December 2000

Abstract

266 nm 1+1 resonance-enhanced multiphoton ionisation has been used in conjunction with a liquid microjet time-of-flight mass (TOF) spectrometer to detect anisole, 4-methoxyphenol and hydroquinone in ethanol solution. We have demonstrated a detection limit of 1 ppm for the parent molecular ion of hydroquinone. A comparison of TOF mass spectra of samples introduced by way of the liquid beam with those entrained in a supersonic free-jet expansion shows that the solute molecules are ionised after evaporation from the surface of the liquid beam. Extensive fragmentation of each parent molecular ion is attributed to excess energy available to the molecules by way of additional photon absorption following the initial photoionisation event. Hydroquinone photoion fragmentation patterns are found to be independent of laser power in the range 2.4–7.1 GW/cm^2, suggesting that saturation of the multiphoton fragmentation channels has been achieved. (Int J Mass Spectrom 207 (2001) 1–12) © 2001 Elsevier Science B.V.

1. Introduction

An in vacuo liquid microjet (LμJ), or "liquid beam," is formed when a liquid sample is injected through a thin aperture or capillary at relatively high speed directly into a vacuum. Liquid beam techniques have gained in popularity over the past decade, with recent advances in the field providing valuable experimental insight into molecular dynamics at the liquid–vacuum interface [1–3]. In an earlier article we reported an extensive investigation into the electrokinetic charging processes occurring in liquid microjets [4]. Faubel and co-workers have measured the kinetic energy distribution of water molecules evaporating from a liquid microjet and have determined that the aqueous liquid microjet is supercooled at its surface [5,6]. Kondow and co-workers have made seminal advances in the coupling of liquid beams with time-of-flight (TOF) mass spectrometry as a tool for investigating laser-induced ion formation and ejection mechanisms at or near the liquid surface [7–17]. Kondow's group has performed a number of experiments showing that UV laser-induced ion formation occurs within the liquid beam, with solvated ions near the liquid surface ejected as clusters into the vacuum by a Coulomb explosion mechanism [18–23]. In a limited number of cases, these workers have also reported solute monomer parent and fragment ions

* Corresponding author. E-mail: mark.buntine@adelaide.edu.au

PII S1387-3806(00)00448-6

that are generated in the gas phase following evaporation from the liquid beam [13,14,18,19,22].

In the last few years liquid beam techniques have been developed to introduce nonvolatile compounds into the gas phase for mass spectrometric interrogation. One motivation for this development has been to overcome the problem of thermal decomposition of many low- or nonvolatile compounds when heated, in attempts to introduce these species into the gas phase. Brutschy and co-workers have employed a liquid beam as the interface between a liquid chromatograph and a TOF mass spectrometer to study the stability of noncovalent complexes, including polypeptides [24–26] and macrocyclic ionophores [27] as well as other biomolecular systems [28,29] and solute–solvent interactions [30–32]. Brutschy and co-workers use a moderate-to-high powered pulsed IR laser to rapidly heat the liquid beam and drive pre-formed ions into the vacuum. Very recently Kondow's group have extended their work to investigate the gas-phase microsolvation dynamics of hydrated clusters of the low volatility molecule resorcinol, meta-$C_6H_4(OH)_2$, by means of IR irradiation of an aqueous liquid beam [9,17]. In these experiments neutral resorcinol and its hydrated clusters are liberated from solution prior to subsequent ionisation by a separate UV laser pulse that passes by the liquid beam.

The laser-induced liquid beam ionisation/desorption (LILBID) technique developed by Brutschy's group has been shown to exhibit good sensitivity, detecting species in the concentration range 10^{-3}–10^{-5} M [24,26,27]. However, the technique is directed to the detection and interrogation of preformed ions in solution. Conversely, Kondow's work has demonstrated that the liquid beam technique is well suited to the investigation of a wide variety of chemical species, including neutral molecules, but relatively high solution concentrations of 0.1–0.2 M have typically been used.

In this article we report the results of an investigation that shows that the liquid beam/TOF approach can be used to detect neutral molecules in solution at concentrations as low as 10^{-5} M. We present a 266 nm photoionisation TOF mass spectra for molecules of high volatility, anisole **1**, and low volatility, 4-methoxyphenol (4-MP) **2**, introduced into the vacuum by means of a liquid microjet (LμJ) at concentrations of 10^{-3} M in ethanol. In addition, we demonstrate the detection sensitivity of this experimental technique by presenting 266 nm photoionisation TOF mass spectra of the essentially nonvolatile molecule hydroquinone (HQ) **3** introduced into the vacuum by means of a LμJ at concentrations of 10^{-3}, 10^{-4} and 10^{-5} M in ethanol. The vapour pressures of compounds **1**, **2**, and **3** at 450 K are approximately 1360, 104, and 22 Torr, respectively [33], reducing to approximately 3.6, 0.015, and 0.001 Torr at 298 K [33]. Having presented these data, we discuss possible strategies to improve the detection sensitivity of the LμJ technique in the future.

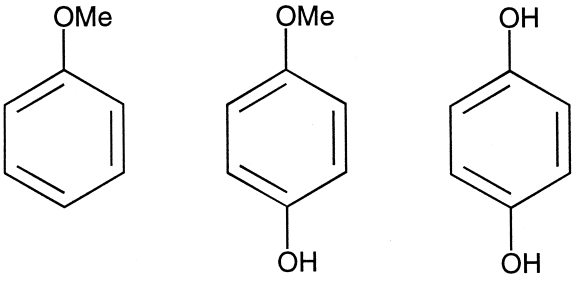

1 **2** **3**

Scheme 1

In order to establish the mechanism for the parent and fragment ion formation, we compare the anisole and hydroquinone LμJ spectra with those generated in a pulsed supersonic expansion. Consistent with earlier results reported by Kondow and co-workers for aniline [14,18,19], anisole [13], and phenol [22], we show that unlike cluster ion formation, ionisation of the solute monomer occurs within an evaporative ensemble released from the surface of the liquid microjet rather than from within the liquid itself.

2. Experimental

A schematic illustration of the LμJ apparatus coupled to a TOF mass spectrometer is presented in

Fig. 1. The apparatus consists of a source chamber (A), a condensation chamber (B), and a TOF chamber (C). The source chamber is equipped with an Edwards Diffstak model 160/700, 700 L/s diffusion pump. The condensation chamber is pumped using two Edwards Model E02, 150 L/s diffusion pumps and the TOF chamber is pumped using a Varian VHS-6 2400 L/s diffusion pump. When the LμJ is in operation, the pressure in the source chamber is typically 10^{-4}–10^{-5} Torr, depending upon the liquid flow rate. Lower source chamber pressures are maintained by cooling a 5 cm diameter copper cup placed above the throat of the diffusion pump with liquid nitrogen (d). Approximately 8 cm downstream from the nozzle the LμJ passes into the condensation chamber. Here, up to three 6×19 cm cylindrical stainless steel traps (e) filled with liquid nitrogen act as cryropumping/condensation units. Typically, the LμJ can be operated for approximately 3 h before the condensation traps need to be removed and cleaned.

The LμJ assembly enters the source chamber by way of a gate valve interlock (f). The LμJ assembly consists of a fused silica capillary tubing of 3 cm in length with a 25 μm internal diameter (g) attached to 0.51 mm internal diameter stainless steel chromatography tubing (h). A constant flow of liquid through the LμJ capillary is supplied and maintained by a conventional liquid chromatography solvent delivery pump (Waters model 590). The pump is fitted with flow dampening modules to minimise oscillations in the flow rate. A 0.2 μm porous filter designed to prevent clogging of the nozzle aperture is placed in series with the flow dampening modules. Liquid flow rates of between 0.2 and 1.0 mL/min are used throughout. Sample solutions of 1 mL are injected into the continuous liquid flow using a Reodyne chromatography injection valve (Model 7725i) fitted with a 1 mL sample loop. The 3 cm channel length of the LμJ capillary (g) allows for laminar flow conditions to be established prior to the liquid jet entering the vacuum chamber [4]. The fused silica tubing is used in these experiments as it is readily available as a gas chromatography consumable, and is relatively inexpensive.

Approximately 12 mm downstream from the nozzle aperture, the LμJ is intersected at right angles (into the plane of the page in Fig. 1) by the focused 266 nm output generated by externally doubling the 532 nm output from a pulsed Nd:YAG laser (Big Sky Laser, ULTRA-CFR). The laser interaction region in Fig. 1 is denoted by an asterisk (*) downstream from the nozzle aperture. The laser output (typically 220–260 μJ/pulse) is focused into the liquid beam by a plano convex lens with a focal length of 250 mm. The diameter of the laser beam incident upon the focusing lens is 5 mm, resulting in a focal spot diameter (i.e. 2×beam waist) of approximately 27 μm [34]. Therefore, the focal spot diameter is ~20% larger than the liquid beam diameter of 25 μm.

The ultraviolet laser radiation ionises solute molecules by way of multiphoton absorption and the nascent solute ions are accelerated out of the source chamber by a two-stage static electric field generated between three ion extraction plates. The first two plates (i and j) are separated by 3 cm. The LμJ aperture is situated midway between these two plates. For the positive ion detection mode discussed here, the rear plate (i) is maintained at +2.5 kV whereas the

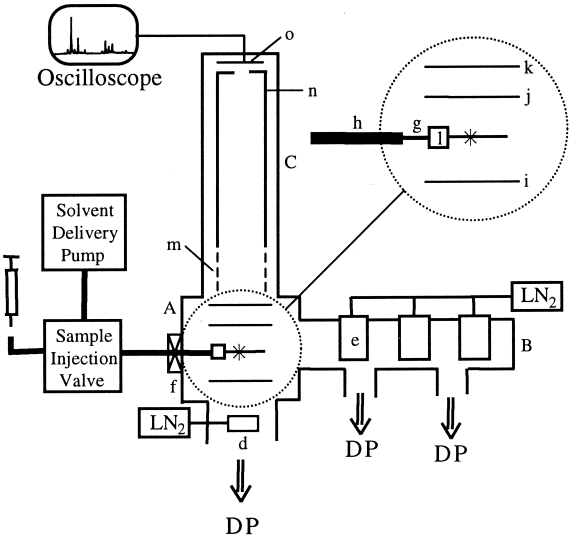

Fig. 1. A schematic illustration of the liquid microjet (LμJ) apparatus coupled to a TOF mass spectrometer. The apparatus consists of a source chamber (A), a condensation chamber (B), and a TOF chamber (C). See text for an explanation of the key features of the instrument and for the details of operation.

middle plate (j) is maintained at +1.2 kV. The third ion plate (k), maintained at ground potential, is separated from the middle plate by another 2 cm. In order to maintain a uniform electric field between the first-stage ion extraction plates, the LμJ capillary passes through a small brass block (l) charged at +2.0 kV. The charged brass block prevents distortions of the ion-extraction field attributable to the electrically grounded fused silica capillary being located between the two charged plates.

Entering the TOF chamber, the fast-moving ions pass through a series of ion focusing and steering optics (m) before traversing a 1 m long field free drift region (n). Ions are detected with a microsphere plate detector (o) (El Mul, MSP-E033A) and their arrival times are measured on a fast digital oscilloscope (LeCroy, model 9350AM, 500 MHz). Resultant mass spectra are routinely collected over 2000 laser pulses.

Gas-phase resonance-enhanced multiphoton ionisation (REMPI) TOF mass spectra are recorded by replacing the liquid microjet source with a pulsed supersonic free-jet expansion aligned co-axially with the TOF detection axis. Anisole vapour is mixed with He seed gas (28 psi) at room temperature behind a pulsed solenoid value (General Valve, Series 9). Hydroquinone solid is packed between layers of glass wool in an in-line reservoir located behind the solenoid valve through which He gas (28 psi backing pressure) is passed. The sample reservoir and solenoid valve are heated to 124°C in order to increase the hydroquinone vapour pressure within the He bath gas.

All LμJ experiments are conducted using once-distilled ethanol as the solvent. All chemicals are used as supplied by the vendor without further purification (hydroquinone, Aldrich, 99%; 4-methoxyphenol, Aldrich, 98%; anisole, Fluka, <99%).

3. Results and discussion

3.1. 266 nm photoionisation of anisole in EtOH

A typical mass spectrum generated following the irradiation of a 10^{-3} M solution of anisole in ethanol with focused 266 nm laser radiation is presented in Fig. 2(a). The laser power was limited to 269 μJ/pulse for the collection of this mass spectrum. The parent ion is clearly visible at $m/z = 108$, with extensive fragmentation evident. The heaviest fragment ion at $m/z=93$ corresponds to the loss of CH_3, with the loss of OCH_3 evident by the fragment at $m/z=77$. Fragment peaks at $m/z = 78$ and 79 correspond to $C_6H_6^+$ and $C_6H_7^+$, respectively. Other groups of hydrocarbon fragment peaks containing five, four, three, and two carbon atoms, respectively, are also present in good abundance, with the C_3H_n, $n = 0–4$, group having the greatest intensity. The lightest fragment peaks correspond to CH_3^+ and C^+; the latter peak indicating that complete fragmentation of a fraction of the parent ions occurs upon photoionisation.

Anisole is ionised by 1+1 resonance-enhanced multiphoton ionisation (1+1 REMPI). At a photon wavelength of 266 nm, the two-photon excitation energy deposited into the neutral parent is 9.34 eV. Therefore, with the ionisation potential of anisole reported to lie in the range 8.18–8.76 eV [35], an upper limit of only 0.58–1.16 eV of excess energy is available to fragment the parent molecular ion, assuming zero kinetic energy of the departing electron. This small amount of excess energy is insufficient to account for the extensive fragmentation observed under the conditions reported here. However, the multiphoton ionisation and dissociation behaviour of benzene and its substituted derivatives is well covered in the literature and can be used to interpret the mass spectrum in Fig. 2(a).

MPI of organic molecules has long been shown to be connected with strong multiphoton dissociation of the molecular ions if the laser power density is high enough [36–38]. The MPI spectrum of benzene was first reported by Johnson in the mid-1970s [39,40] and has subsequently become one of the most extensively studied molecules for elucidating aspects of MPI and fragmentation [37,41,42]. Schlag and co-workers proposed a “ladder-switching” model to explain the relationship between laser power density and the degree of molecular ion fragmentation [43–46]. Complete fragmentation of the benzene molecular ion is observed with the formation of C^+ fragment ions using nanosecond lasers and medium power densities

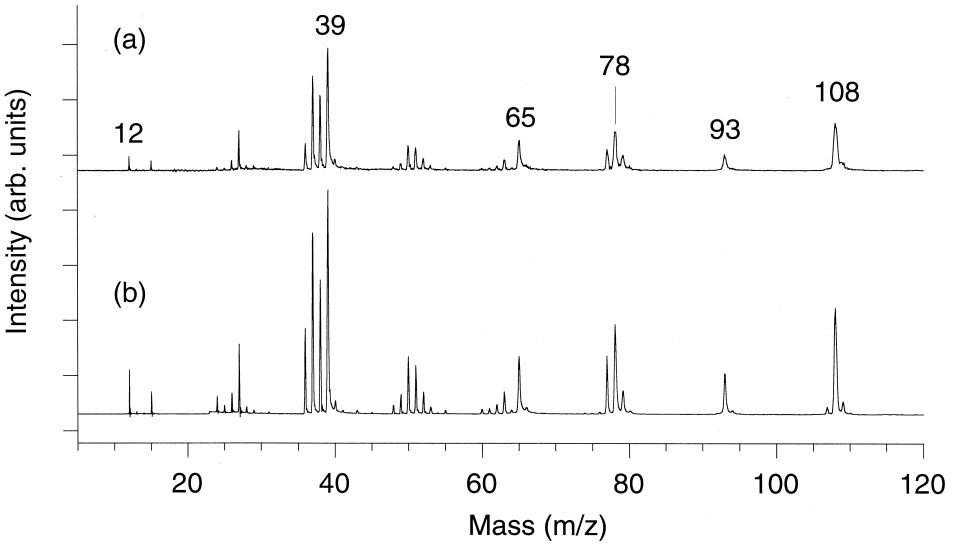

Fig. 2. (a) Liquid beam/TOF 1+1 REMPI mass spectrum of a 10^{-3} M solution of anisole in ethanol recorded using 269 μJ pulses of 266 nm laser radiation (2.9 GW/cm^2). (b) Gas-phase TOF 1+1 REMPI mass spectrum of anisole vapour seeded at room temperature into a helium supersonic expansion. This spectrum was recorded using 221 μJ pulses of 266 nm laser radiation (2.4 GW/cm^2).

(<10 GW/cm^2) [47]. The general conclusion from this extensive body of work is that for power densities less than approximately 10 GW/cm^2, molecular ionisation precedes dissociation, with up to four photons being absorbed by the molecular ion leading to complete molecular fragmentation [41,42].

The 266 nm REMPI mass spectrum of anisole has been reported by Chang and Johnson with a laser fluence of ~10 MW/cm^2 [48]. These workers found only a moderate amount of parent ion fragmentation, with the lightest fragment ion observed at $m/z = 65$, corresponding to $C_5H_5^+$. These workers attributed the formation of fragment ions at $m/z = 93$, 79, 78, and 65 to the absorption of only one additional photon following the ionisation event. The interpretation of Chang and Johnson is consistent with the reported appearance potentials of the relevant fragment ions from anisole [35]. By contrast, the REMPI spectrum presented in Fig. 2(a) displays considerably greater molecular fragmentation than reported by Chang and Johnson. The presence of the C^+ fragment ion indicates that complete fragmentation is occurring for some of the anisole parent. The mass spectrum in Fig. 2(a) was collected with a laser power density of ~3 GW/cm^2. Based upon the fragmentation behaviour of benzene discussed previously, our observation of complete fragmentation of a fraction of the anisole molecules at a laser fluence of 3 GW/cm^2 is not unexpected. At 3 GW/cm^2, the laser power density is sufficiently high to facilitate the absorption of up to four additional photons following ionisation.

Having discussed the extent of fragmentation in the anisole LμJ mass spectrum, some consideration needs to be given to the mechanism of fragment ion formation from anisole originating as a solute within the liquid microjet. The anisole fragment ions can conceivably be generated by three possible mechanisms. The first possibility is that solute molecules within the liquid beam are photoionised, with the resulting intact parent molecular ions being ejected from the liquid beam prior to fragmentation occurring in the gas phase. This mechanism of slow fragmentation following Coulomb ejection into the gas phase seems improbable because the considerable amount of excess energy deposited into the anisole parent will result in rapid fragmentation within the liquid beam following photoexcitation. Moreover, although the mass spectrum in Fig. 2(a) contains peaks with some asymmetry, the spectrum presents no compelling evidence for metastable ion decay within the TOF

drift region. The second ion formation possibility is that ionisation and fragmentation occur within the liquid beam with the subsequent Coulomb ejection of all ions on or near the liquid surface. The Coulomb ejection model has been described extensively by Kondow and co-workers [18–23]. Under the Coulomb ejection conditions it is likely that different fragment ions will interact with the ethanol solvent to differing extents, yielding a mass spectrum intensity distribution that tells us something about the extent of these fragment ion-solvent interactions. The third ion formation possibility is that anisole evaporates from the liquid beam with the resultant vapour subsequently ionised within the laser ionisation volume. Under these conditions the ion fragmentation intensity pattern would be expected to be indistinguishable from that obtained in a gas-phase photoionisation mass spectrum.

The 266 nm 1+1 REMPI TOF mass spectrum of anisole generated in a pulsed supersonic expansion is presented in Fig. 2(b). This photoionisation mass spectrum was generated with a laser power of 221 μJ/pulse (2.4 GW/cm^2) and is essentially identical in appearance to the mass spectrum presented in Fig. 2(a), providing compelling evidence for the scenario in which anisole solute evaporates from the liquid beam prior to laser ionisation. In the LμJ source, if fragment ions were formed in solution it would be expected that ion–solvent interactions would result in a differing fragment ion intensity pattern to that generated in the gas phase.

When the ionisation laser irradiates outside the liquid beam by translating the laser focal point 5 mm (more than 150 laser focal spot diameters) in the direction toward the TOF chamber, an almost identical mass spectrum to that presented in Fig. 2(a) is obtained, providing further evidence in support of the evaporative model. Interestingly, if the ionisation laser is translated 5 mm away from the TOF chamber a degraded mass spectrum (both in terms of resolution and ion intensity) results, presumably because the photoions interact with the liquid beam as they are accelerated out of the source chamber.

Evaporation from the surface of liquid beams has been previously reported. For example, the molecular velocity distribution of H_2O molecules evaporating from the surface of a liquid beam of water has been reported by Faubel et al. [5]. In work more closely related to that reported here, Kondow and co-workers have photoionised solute aniline molecules in the gas phase that have been attributed to evaporation from a propanol liquid beam [18]. Nonetheless, there have been only a few reports in the literature describing evaporation from small diameter liquid jets [49,50], and further work is required in this area to more fully characterise the mechanistic details of evaporation into a vacuum.

Careful comparison of the mass spectra presented in Fig. 2(a) and (b) reveals that the peak widths of ions generated in the gas-phase region surrounding the liquid beam are broader than those generated in the pulsed supersonic free jet. The added width of the peaks in the LμJ mass spectrum can most likely also be ascribed to interactions between the nascent gas-phase photoions and the liquid jet as the ions are accelerated towards the TOF mass spectrometer. Recall that the laser focal spot diameter is approximately 27 μm which is ~20% larger than the diameter of the liquid beam at 25 μm. Therefore, photoions generated behind the liquid beam (away from the TOF analyser) will interact with the liquid beam to a greater extent than those generated in front of the liquid beam (toward the TOF analyser). The differing degrees of interaction with the liquid beam will result in some peak broadening.

3.2. 266 nm photoionisation of 4-methoxyphenol in EtOH

A typical mass spectrum generated following the irradiation of a 10^{-3} M solution of 4-methoxyphenol (4-MP) in ethanol with focused 266 nm laser radiation is presented in Fig. 3. The laser power was limited to 227 μJ/pulse (2.5 GW/cm^2) for the collection of this mass spectrum. 4-MP has a room temperature vapour pressure approximately two orders of magnitude lower than that of anisole [33]. 4-MP is also ionised by a 1+1 REMPI process. The ionisation potential for 4-MP is reported to lie between 7.5 and 8.02 eV [35], leaving a maximum of between 1.3 and 1.8 eV of

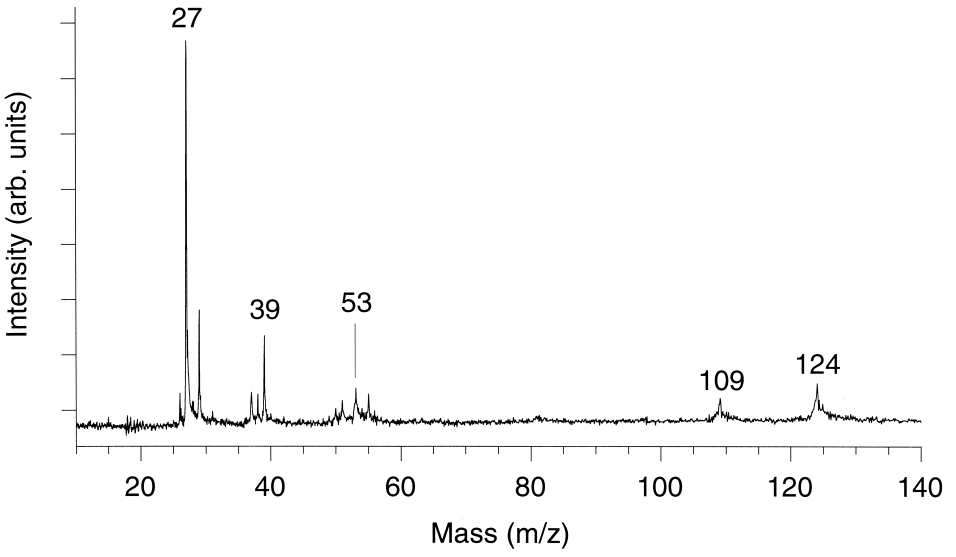

Fig. 3. Liquid beam/TOF 1+1 REMPI mass spectrum of a 10^{-3} M solution of 4-methoxyphenol in ethanol recorded using 227 μJ pulses of 266 nm laser radiation (2.5 GW/cm^2).

excess energy available to the parent ion following two-photon ionisation. Extensive fragmentation is evident in the mass spectrum in Fig. 3, with a small parent ion at $m/z = 124$ and the most intense fragment at $m/z = 27$ corresponding to $C_2H_3^+$. Brown [51] has reported appearance potentials for heavy mass fragments around 11 eV. The presence of heavy mass fragments would indicate that only one additional photon is being absorbed following the ionisation event. However, these species do not dominate the mass spectrum in Fig. 3. It is therefore evident that between two and three additional photons are absorbed by the parent molecular ion following the initial ionisation event. Compared to the anisole mass spectrum in Fig. 2(a), the lack of C^+ in the mass spectrum in Fig. 3 may suggest that a fourth photon is not absorbed following ionisation. An alternative explanation is that absorption of a fourth photon is required to generate the fragment ions around $m/z = 27$ but that the C^+ formation channel(s) has (have) a low propensity. As will be discussed in the next section, this latter scenario appears to apply to the photoionisation of hydroquinone.

The absorption spectrum of 10^{-4} M 4-MP in ethanol shows a broad absorption feature in the range 315–245 nm, with a maximum at 287 nm [52]. The gas-phase absorption spectrum, recorded with 4-MP vapour in a static cell at 335 K, is similar to that in ethanol solution [52], with a small shift in the absorption band of ~3 nm to the red. At 266 nm both the solution and gas-phase absorption intensities are approximately 60% of their maxima. The absorption intensities at 300 nm are also approximately 60% of their maxima, indicating that this longer wavelength has a comparable one-photon absorption cross section to that at 266 nm. With an ionisation potential reported to lie between 7.5 and 8.02 eV, we therefore expect that at the laser powers employed in this study, two-photon ionisation of 4-MP at a laser wavelength of approximately 300 nm (4.1 eV) should proceed with a similar propensity to that at 266 nm. However, even with two to three photons absorbed following ionisation, the lower energy of each photon should result in less fragmentation and hence a greater mass spectral detection sensitivity for the parent ion.

Our experiment is currently only equipped with the fixed-frequency 266 nm quadrupled output from a pulsed Nd:YAG laser. Tunable wavelength excitation experiments designed to explore fragmentation pathways and extend the detection sensitivity of this

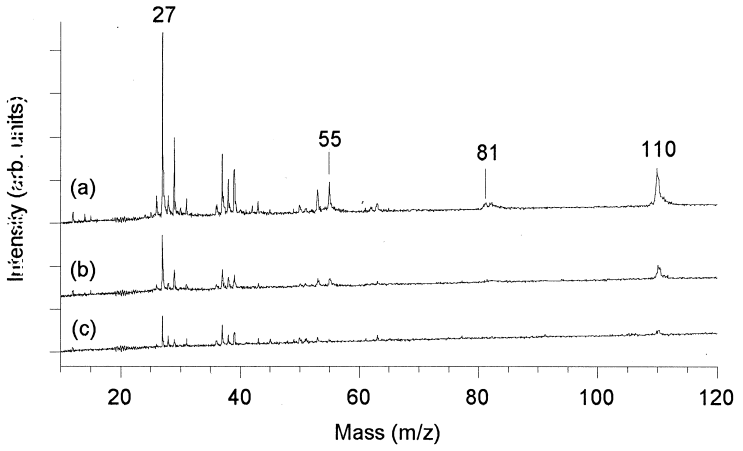

Fig. 4. Liquid beam/TOF 1+1 REMPI mass spectra of solutions of hydroquinone in ethanol recorded using 256 μJ pulses of 266 nm laser radiation (2.8 GW/cm^2). (a) 10^{-3} M (110 ppm), (b) 10^{-4} M (11.0 ppm), and (c) 10^{-5} M (1.10 ppm).

technique are planned for the near future. The obvious point to keep in mind from this work is that 266 nm 1+1 REMPI is not necessarily suited as a generic photoionisation method. Rather, a tunable photoionisation source should allow for better detection sensitivity of a wider range of aromatic parent solute ions.

3.3. 266 nm photoionisation of hydroquinone in EtOH

The liquid beam technique described here is perhaps best suited to the mass spectrometric detection of nonvolatile neutral molecules in solution where other commonly used techniques lack the required detection sensitivity. Hydroquinone (HQ) has a very small room temperature vapour pressure of ~0.001 Torr [33] (cf. ~0.015 Torr for 4-MP and ~3.6 Torr for anisole) and is therefore an excellent candidate to test the detection sensitivity of this experimental technique. Mass spectra generated following the focused 266 nm irradiation of 10^{-3}, 10^{-4}, and 10^{-5} M HQ in ethanol are presented in Fig. 4(a), (b), and (c), respectively. The mass spectrum recorded at a concentration of 10^{-5} M corresponds to a parent ion detection limit of 1.1 ppm. All spectra in Fig. 4 were collected with a laser power of 256 μJ/pulse (2.8 GW/cm^2).

The mass spectra in Fig. 4 clearly show the parent molecular ion at $m/z = 110$. Extensive fragmentation is evident, with the most intense peaks in each mass spectrum corresponding to $C_2H_3^+$ ions at $m/z = 27$. The C^+ fragment ion is present in small yield, suggesting that complete fragmentation to atomic ions is not a dominant process. An investigation into the stepwise ionisation of HQ in a static cell by means of TOF mass spectrometry has recently been reported by Feofilov and co-workers [53]. These workers ionised HQ vapour in the range 315–275 nm and found that at laser powers less than ~10 MW/cm^2 the TOF mass spectra are dominated by the presence of the parent molecular ion. Indeed, there is almost no evidence for any molecular fragmentation at all under these low laser power conditions. Conversely, at higher laser powers (up to ~100 MW/cm^2) extensive fragmentation similar to that observed in the mass spectra in Fig. 4 is evident. Feofilov and co-workers explore the dynamics of the HQ photoionisation process and conclude that apart from fragmentation occurring in a stepwise manner following the initial ionisation event (Schlag's ladder-switching model), formation of the light fragment ions at $m/z = 26$–29 requires the absorption of at least 4 additional photons following ionisation. We must therefore conclude that at the higher laser powers employed in our study at least four additional photons following ionisation are being absorbed.

In Fig. 5 we present a series of 266 nm 1+1

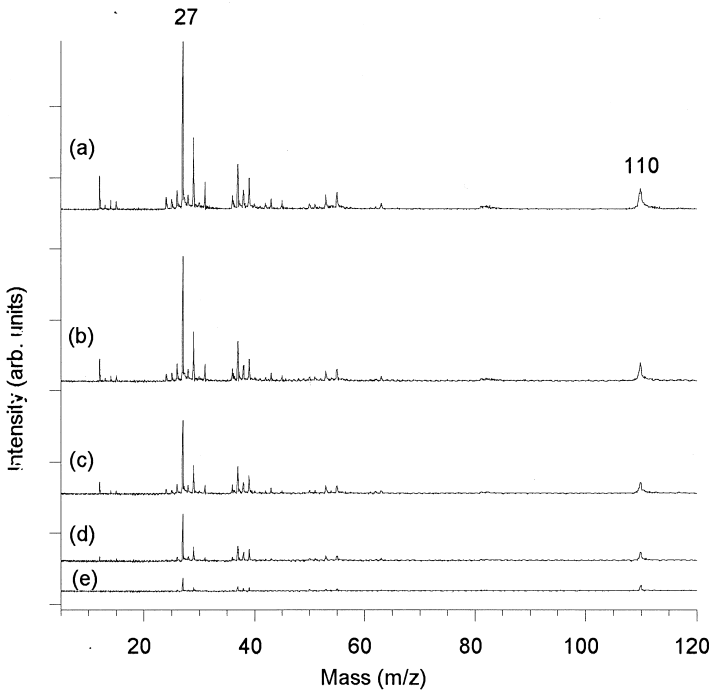

Fig. 5. Liquid beam/TOF 1+1 REMPI mass spectra of a 10^{-3} M solutions of hydroquinone in ethanol recorded using (a) 646 μJ pulses (7.1 GW/cm^2), (b) 483 μJ pulses (5.3 GW/cm^2), (c) 344 μJ pulses (3.8 GW/cm^2), (d) 253 μJ pulses (2.8 GW/cm^2), and (e) 221 μJ pulses (2.4 GW/cm^2) of 266 nm laser radiation.

REMPI mass spectra of 10^{-3} M HQ in an ethanol liquid beam. Laser powers vary by a factor of ~3, ranging from 221 μJ/pulse (2.4 GW/cm^2) to 646 μJ/pulse (7.1 GW/cm^2). Clearly the magnitude of the ion signal increases with laser power, but over the laser power range investigated, the fragmentation intensity patterns remain essentially unchanged. The lack of variation in the REMPI mass spectra, combined with the fact that mass spectra with a similar appearance have been reported by Feofilov and coworkers at laser powers ~100 times lower than those reported here [53] suggest that the multiphoton fragmentation channels have been saturated. The increased ion yield as a function of laser power density is attributable to the initial two-photon ionisation step, not any subsequent processes. Indeed, it is unlikely that the HQ parent molecular ion or any daughter fragment ions are absorbing more than four "post-ionisation" photons. Under saturation conditions we must conclude that C^+ is not a dominant fragment ion in the HQ 266 nm REMPI spectrum because fragmentation channels that lead to the formation of this ion have a weak relative propensity.

Even though HQ has a significantly lower vapour pressure than 4-MP or anisole, the 1+1 REMPI mass spectra presented in Fig. 5 still arise from photoionisation of gas-phase molecules that have evaporated from the surface of the liquid beam and are present in the laser ionisation volume. Indeed, an almost identical mass spectrum is generated when the ionisation laser irradiates outside the liquid beam, confirming the evaporative model. However, unlike other gas-phase studies of HQ where the sample is initially heated to between 80 and 200 °C in order to obtain sufficient number densities for spectroscopic interrogation [53–58], the mass spectra in Fig. 5 are collected from gas-phase molecules maintained at or slightly below room temperature. Temperatures lower than ambient may be achieved because even though the liquid beam in these studies is created from

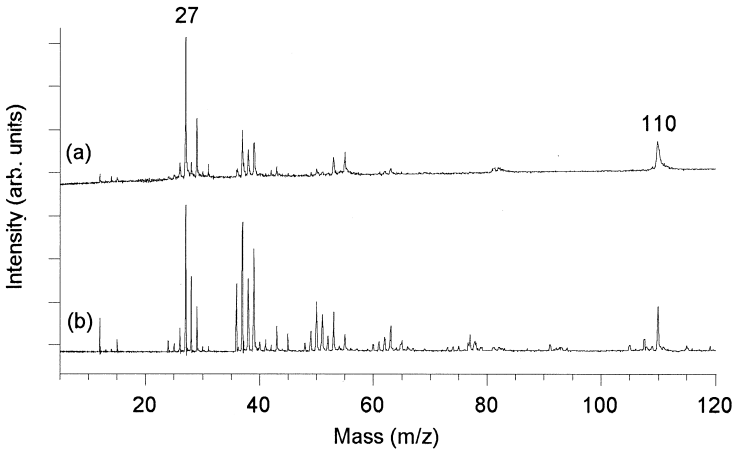

Fig. 6. (a) Liquid beam/TOF 1+1 REMPI mass spectrum of a 10^{-3} M solution of hydroquinone in ethanol recorded using 256 μJ pulses of 266 nm laser radiation (2.8 GW/cm^2). (b) Gas-phase TOF 1+1 REMPI mass spectrum of hydroquinone vapour seeded at 124 °C into a helium supersonic expansion. This spectrum was recorded using 222 μJ pulses of 266 nm laser radiation (2.4 GW/cm^2).

samples equilibrated to the laboratory temperature of 20 °C, endothermic evaporation will lower the temperature of the liquid beam itself. As a result, the molecules evaporating from the liquid surface should possess a thermal energy distribution lower than ambient. Indeed, Faubel and co-workers have previously determined that evaporation of water results in supercooled aqueous liquid beams with solution temperatures less than 210 K [5,6].

In Fig. 6 we compare the gas-phase 266 nm 1+1 REMPI mass spectra of HQ recorded under LμJ [Fig. 6(a)] and supersonic free jet [Fig. 6(b)] conditions. The former spectrum was recorded at a solute concentration of 10^{-3} M HQ in ethanol with a laser power of 256 μJ/pulse (2.8 GW/cm^2). The latter spectrum was recorded with the sample heated to 124 °C behind the nozzle and with a laser power of 222 μJ/pulse (2.4 GW/cm^2). As with the mass spectra presented in Fig. 2, the LμJ spectrum exhibits slightly broader peak widths compared to the free jet spectrum. As with anisole, we ascribe these differences in peak widths to the fact that ions generated in the vicinity of the liquid beam interact with the liquid as they are accelerated into the TOF drift region. However, unlike the spectra presented in Fig. 2, the spectra in Fig. 6, while broadly similar, show significant differences in their fragmentation patterns. It is unclear whether these differences can be attributed to the fact that the HQ sample is initially heated prior to cooling in the supersonic expansion. Further work will be required, including ionisation at longer wavelengths, to explore this issue.

4. Conclusions

We have used 266 nm 1+1 REMPI together with a liquid microjet/TOF mass spectrometer to detect nonvolatile aromatic species in solution. We have demonstrated a detection limit of 1.1 ppm for the parent molecular ion of hydroquinone. A comparison of TOF mass spectra of samples introduced by way of the liquid beam with those entrained in a supersonic free-jet expansion shows that that solute molecules are ionised after evaporation from the surface of the liquid beam. Extensive fragmentation of the parent molecular ions is attributed to the excess energy available to the molecules following additional photon absorption after the initial photoionisation event. Our results indicate that liquid beam mass spectrometry has significant potential as an experimental technique for exploring the photochemical behaviour of low- or nonvolatile compounds at non-elevated temperatures.

Acknowledgements

This work was supported by the University of Adelaide, the South Australian Department of Mines and Energy through the State Energy Research Advisory Committee (SENRAC), and the Australian Land and Water Resources Research and Development Corporation (LWRRDC). The technical support provided by the University of Adelaide Mechanical, Electronics and Glassblowing Workshops is gratefully acknowledged. W.L.H. acknowledges the support of a University of Adelaide postgraduate scholarship.

References

[1] M. Faubel, T. Kisters, Nature 339 (1989) 527.
[2] M. Faubel, B. Steiner, Ber. Bunsenges. Phys. Chem. 96 (1992) 1167.
[3] M. Faubel, B. Steiner, J.P. Toennies, Mol. Phys. 90 (1996) 327.
[4] W.L. Holstein, L.J. Hayes, E.M.C. Robinson, G.S. Laurence, M.A. Buntine, J. Phys. Chem. B 103 (1999) 3035.
[5] M. Faubel, S. Schlemmer, J.P. Toennies, Z. Phys. D 10 (1988) 269.
[6] M. Faubel, B. Steiner, J.P. Toennies, J. Chem. Phys. 106 (1997) 9013.
[7] N. Horimoto, F. Mafuné, T. Kondow, J. Phys. Chem. 100 (1996) 10046.
[8] N. Horimoto, F. Mafuné, T. Kondow, Chem. Lett. (1997) 159.
[9] N. Horimoto, J. Kohno, F. Mafuné, T. Kondow, J. Phys. Chem. A 103 (1999) 9569.
[10] J. Kohno, F. Mafuné, T. Kondow, J. Am. Chem. Soc. 116 (1994) 9801.
[11] J. Kohno, N. Horimoto, F. Mafuné, T. Kondow, J. Phys. Chem. 99 (1995) 15627.
[12] J. Kohno, F. Mafuné, T. Kondow, J. Phys. Chem. A 104 (2000) 1079.
[13] F. Mafuné, J. Kohno, T. Nagata, T. Kondow, Chem. Phys. Lett. 218 (1994) 7.
[14] F. Mafuné, Y. Takeda, T. Nagata, T. Kondow, Chem. Phys. Lett. 218 (1994) 234.
[15] F. Mafuné, J. Kohno, T. Kondow, J. Phys. Chem. 100 (1996) 4476.
[16] H. Matsumura, F. Mafuné, T. Kondow, J. Phys. Chem. 99 (1995) 5861.
[17] N. Horimoto, J. Kohno, F. Mafuné, T. Kondow, Chem. Phys. Lett. 318 (2000) 536.
[18] J. Kohno, F. Mafuné, T. Kondow, J. Phys. Chem. A 104 (2000) 243.
[19] F. Mafuné, Y. Takeda, T. Nagata, T. Kondow, Chem. Phys. Lett. 199 (1992) 615.
[20] F. Mafuné, J. Kohno, T. Kondow, J. Phys. Chem. 100 (1996) 10041.
[21] F. Mafuné, J. Kohno, T. Kondow, J. Chin. Chem. Soc. 42 (1995) 449.
[22] F. Mafuné, Y. Hashimoto, M. Hashimoto, T. Kondow, J. Phys. Chem. 99 (1995) 13814.
[23] F. Mafuné, Y. Hashimoto, T. Kondow, Chem. Phys. Lett. 274 (1997) 127.
[24] W. Kleinekofort, A. Pfenninger, T. Plomer, C. Griesinger, B. Brutschy, Int. J. Mass Spectrom. Ion Processes 156 (1996) 195.
[25] W. Kleinekofort, J. Avdiev, B. Brutschy, Int. J. Mass Spectrom. Ion Processes 152 (1996) 135.
[26] A. Wattenberg, H.-D. Barth, B. Brutschy, J. Mass Spectrom. 32 (1997) 1350.
[27] F. Sobott, W. Kleinekofort, B. Brutschy, Anal. Chem. 69 (1997) 3587.
[28] A. Wattenberg, F. Sobott, B. Brutschy, Rapid Commun. Mass Spectrom. 14 (2000) 859.
[29] W. Kleinekofort, M. Schweitzer, J.W. Engels, B. Brutschy, Int. J. Mass Spectrom. Ion Processes 163 (1997) 1L.
[30] F. Sobott, S.A. Schunk, F. Schüth, B. Brutschy, Chem. Eur. J. 4 (1998) 2353.
[31] A. Wattenberg, F. Sobott, H.-D. Barth, B. Brutschy, Eur. Mass Spectrom. 5 (1999) 71.
[32] F. Sobott, A. Wattenberg, W. Kleinekofort, A. Pfenninger, B. Brutschy, Fresenius, J. Anal. Chem. 360 (1998) 745.
[33] C.L. Yaws, Handbook of Vapor Pressure, Gulf Publishing, Houston, TX, 1994, Vol. 3.
[34] A.E. Siegman, Lasers, University Science Books, Mill Valley, CA, 1986.
[35] NIST Chemistry WebBook, http://webbook.nist.gov/chemistry.
[36] P.M. Johnson, C.E. Otis, Annu. Rev. Phys. Chem. 32 (1981) 139.
[37] D.A. Gobeli, J.J. Yang, M.A. El-Sayed, Chem. Rev. 85 (1985) 529.
[38] K.W.D. Ledingham, D.J. Smith, R.P. Singhal, T. McCanny, P. Graham, H.S. Kilic, W.X. Peng, A.J. Langley, P.F. Taday, C. Kosmidis, J. Phys. Chem. A 103 (1999) 2952.
[39] P.M. Johnson, J. Chem. Phys. 62 (1975) 4562.
[40] P.M. Johnson, J. Chem. Phys. 64 (1976) 4143.
[41] L. Zandee, R.B. Bernstein, J. Chem. Phys. 71 (1979) 1359.
[42] P. Hering, A.G.M. Maaswinkel, K.L. Kompa, Chem. Phys. Lett. 83 (1981) 222.
[43] W. Dietz, H.J. Neusser, U. Boesl, E.W. Schlag, Chem. Phys. 66 (1982) 105.
[44] U. Boesl, H.J. Neusser, E.W. Schlag, J. Chem. Phys. 72 (1980) 4327.
[45] U. Boesl, H.J. Neusser, E.W. Schlag, Chem. Phys. Lett. 87 (1982) 1.
[46] U. Boesl, R. Weinkauf, K. Walter, C. Weickhardt, E.W. Schlag, J. Phys. Chem. 94 (1990) 8567.
[47] U. Boesl, R. Weinkauf, K. Walter, C. Weickhardt, E.W. Schlag, Ber. Bunsenges. Phys. Chem. 94 (1990) 1357.
[48] T.-C. Chang, M.V. Johnson, J. Phys. Chem. 91 (1987) 884.
[49] T.A. Kowalewski, W.J. Hiller, Phys. Fluids A 5 (1993) 1883.

[50] C.J.H. Knox, L.F. Phillips, J. Phys. Chem. B 102 (1998) 10515.
[51] P. Brown, Org. Mass Spectrom. 4 (1970) 519.
[52] The absorption spectra of 4-methoxyphenol in ethanol and in the gas phase at 335 K were recorded using a Carey Model 300 UV-visible spectrometer.
[53] M.E. Akopyan, V.I. Kleimenov, A.G. Feofilov, High Energy Chem. 34 (2000) 107.
[54] C.H. Sin, R. Tembreull, D.M. Lubman, Anal. Chem. 56 (1984) 2776.
[55] T.M. Dunn, R. Tembreull, D.M. Lubman, Chem. Phys. Lett. 121 (1985) 453.
[56] G.N. Patwari, S. Doraiswamy, S. Wategaonkar, Chem. Phys. Lett. 289 (1998) 8.
[57] S.J. Humphrey, D.W. Pratt, J. Chem. Phys. 99 (1993) 5078.
[58] W. Caminati, S. Melandri, J. Chem. Phys. 100 (1994) 8569.